Functional Analysis of the Copper-Dependent Quercetin 2,3-Dioxygenase. 2. X-ray Absorption Studies of Native Enzyme and Anaerobic Complexes with the Substrates Quercetin and Myricetin†

Roberto A. Steiner,‡ Wolfram Meyer-Klaucke,*,§ and Bauke W. Dijkstra*,‡

Laboratory of Biophysical Chemistry, Department of Chemistry, University of Groningen, Nijenborgh 4, 9747 AG Groningen, The Netherlands, and European Molecular Biology Laboratory, c/o DESY, Notkestrasse 85, D-22603 Hamburg, Germany

Received November 26, 2001; Revised Manuscript Received May 7, 2002

ABSTRACT: Quercetin 2,3-dioxygenase (2,3QD) is a mononuclear copper-dependent dioxygenase which catalyzes the cleavage of the heterocyclic ring of the flavonol quercetin (5,7,3′,4′-tetrahydroxy flavonol) to produce 2-protocatechuoyl-phloroglucinol carboxylic acid and carbon monoxide. In this study, X-ray absorption spectroscopy has been used to characterize the local structural environment of the Cu^{2+} center of *Aspergillus japonicus* 2,3QD. Analysis of the EXAFS region of native 2,3QD at functionally relevant pH (pH 6.0) indicates an active site equally well-described by either four or five ligands (3N(His) + 1−2O) at an average distance of 2.00 Å. Bond valence sum analysis confirms that the best model is somewhere between the two. When, however, 2,3QD is anaerobically complexed with its natural substrate quercetin, the copper environment undergoes a transition to a five-coordinated cage, which is also best modeled by a single shell of N/O scatterers at the average distance of 2.00 Å. This coordination is independently confirmed by the anaerobic complex with myricetin (5′-hydroxy quercetin). XANES analysis confirms that substrate binding does not reduce the Cu^{2+} ion. The present study gives the first direct insights into the coordination chemistry of the enzyme complexed with its substrates. It suggests that activation for O_2 attack is achieved by monodentate substrate complexation to the copper ion through the 3-hydroxyl group. In addition, monodentate carboxylate ligation by the Glu73 side chain is likely to play a role in the fine-tuning of the equilibrium leading to the formation of the activated E·S complex.

Dioxygenases are ubiquitous enzymes which catalyze the transfer of both atoms of molecular oxygen into a substrate. They play an important role in the biosynthesis and catabolism of various metabolites and in several detoxification mechanisms (*1*). In particular, dioxygenases are essential mediators in the difficult degradation process of aromatic compounds (*1*, *2*). As a consequence of the triplet ground state of molecular oxygen, dioxygenases often rely on the presence of a metallic cofactor to catalyze the transformation of singlet ground-state organic substrates (*3*). The most commonly employed metal is non-heme iron (*4*). However, enzymes containing other metallocenters (Cu, Mn, Mg) have also been reported (*5*−*7*).

Quercetin 2,3-dioxygenase (2,3QD)[1] is the only dioxygenase unambiguously known to depend on copper (*7*−*9*). The enzyme is produced in *Pullularia* (*10*), *Fusarium* (*11*), and *Aspergillus* (*12*) species when grown on rutin (quercetin 3-rhamnoglucoside) as a carbon source. In the degradative pathway of rutin the action of 2,3QD follows that of the esterase rutinase which releases quercetin from the glycoside (*13*). 2,3QD catalyzes the cleavage of the O-heteroaromatic ring of the flavonol quercetin (5,7,3′,4′-tetrahydroxy flavonol, QUE) to 2-protocatechuoyl-phloroglucinol carboxylic acid and carbon monoxide (Figure 1). The specificity of 2,3QD is not limited to QUE. In their study of *Aspergillus flavus* 2,3QD, Oka et al. (*14*) discovered that the enzyme is able to catalyze the disruption of several polyphenolic flavonols. The rate at which they are degraded has been found to be influenced by the OH topology at the A- and B-rings. In general, the presence of 4′- or 7-hydroxy groups increases the rate of cleavage and decreases the Michaelis constant (*14*). As a result, quercetin is processed about 2000 times faster than flavonol (3-hydroxy flavone). Myricetin (5,7,3′,4′,5′-pentahydroxy flavonol, MYR), which possesses an additional meta 5′-OH group at the B-ring, is the substrate closest to QUE. It is processed only marginally slower (1.2 times).

2,3QD is the only non-iron dioxygenase for which a crystal structure is known. (*9*). The 1.6 Å resolution X-ray structure of the enzyme from *Aspergillus japonicus* solved at pH 5.2 shows that the enzyme is a glycosylated homodimer of about 100 kDa containing one copper ion per monomer (350 amino acids). The mononuclear copper center displays a double

† The research described here was supported by The Netherlands Foundation for Chemical Research (CW) with financial aid from The Netherlands Foundation for Scientific Research (NWO). The EU supported the work at the EMBL outstation at DESY, Hamburg, through the HCMP Access to Large Installations Program.

* Corresponding author. Phone (Bauke W. Dijkstra): +31-50-3634381. Fax: +31-50-3634800. E-mail: bauke@chem.rug.nl.

‡ University of Groningen.

§ European Molecular Biology Laboratory.

[1] Abbreviations: 2,3QD, quercetin 2,3-dioxygenase; E·S, enzyme·flavonol complex; EXAFS, extended X-ray absorption fine structure; MYR, myricetin (5,7,3′,4′,5′-pentahydroxy flavonol); QUE, quercetin (5,7,3′,4′-tetrahydroxy flavonol); XANES, X-ray absorption near edge structure; XAS, X-ray absorption spectroscopy.

10.1021/bi015974y CCC: $22.00
Published on Web 06/01/2002

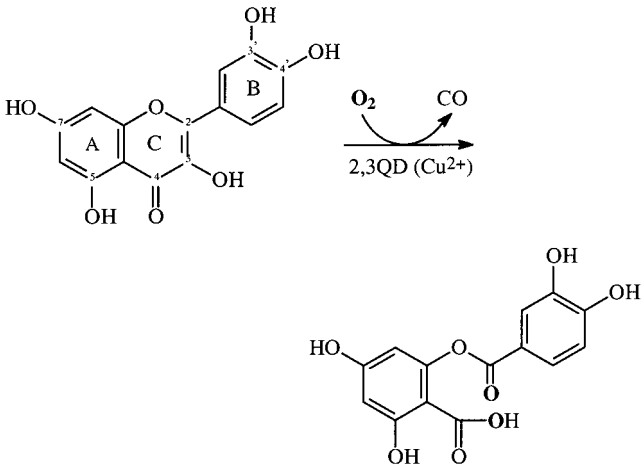

FIGURE 1: Scheme of 2,3QD-mediated dioxygenation of the substrate quercetin (5,7,3′,4′-tetrahydroxy flavonol). Atom nomenclature is indicated in the substrate.

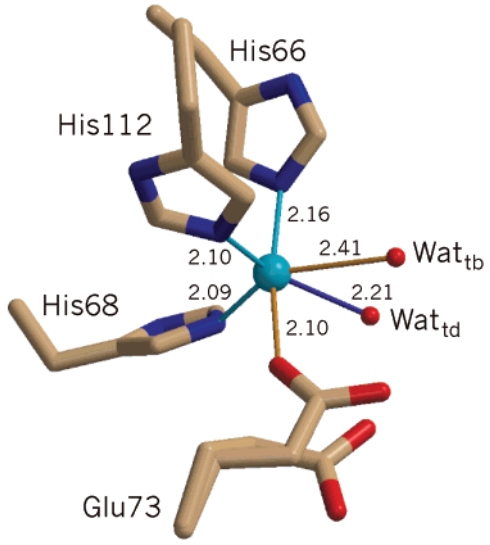

FIGURE 2: Copper coordination in 2,3QD as derived from the crystal structure (PDB code 1JUH) (*9*). Two geometries are present: a distorted tetrahedral (coordination ~70% of the total) with His66, His68, His112, and Wat_{td} as ligands and a trigonal bipyramidal coordination with a strong square pyramidal component (τ index (*32*) = 0.63) formed by the same histidine residues, Wat_{tb} and Glu73. The apical ligands of the latter are His66 and Glu73. All histidine residues coordinate through their $N^{\epsilon 2}$ atoms while Glu73 is bound in a syn-monodentate fashion through its $O^{\epsilon 1}$ atom. Averaged metal−ligand distances (average calculated over the four molecules present in the crystallographic asymmetric unit) are given in Å. This figure was generated with the program MOLSCRIPT (*33*) and rendered with the program RASTER3D (*34*).

coordination (Figure 2). One coordination is pseudo-tetrahedral with three histidine residues (His66, His68, and His112) and a water molecule (Wat_{td}) as ligands. The other coordination is mixed trigonal bipyramidal/square pyramidal and has the same histidine residues, a solvent molecule (Wat_{tb}), and the carboxylate side chain of Glu73 as ligands. The different positions of Wat_{td} and Wat_{tb} and the double conformation of Glu73 determine the two different coordination geometries. Glu73 coordinates the metal only in its minor conformation. In its principal conformation, the carboxylate side chain points away from the metal center.

The early biochemical studies on *A. flavus* 2,3QD (*14*) and extensive biomimetic synthetic work (*15*−*21*) have led to the proposal that the formation of a 2,3QD·flavonol complex constitutes the first catalytic step. However, no structural data for such a complex is as yet available. Instead, its existence has even been challenged by the finding that the anaerobic addition of QUE to *A. niger* 2,3QD did not result in any changes in the EPR spectrum (*8*). To investigate this in more detail, we have undertaken an X-ray absorption spectroscopic study on *A. japonicus* 2,3QD in solution at functionally relevant pH (6.0). The vantage point given by the knowledge of the crystal structure of this enzyme provided a good platform for the refinement of the native EXAFS data which, in turn, resulted in a properly calibrated initial ligand set for the characterization of the 2,3QD·QUE and 2,3QD·MYR complexes.

MATERIALS AND METHODS

Sample Preparation. 2,3QD was purified as previously described (*9*). Protein purity was ascertained by SDS−PAGE gel electrophoresis. For XAS measurements, a glycosylated form of the enzyme was used (~25% w/w sugar content). EXAFS samples were concentrated in Centricon concentrators (Amicon Inc., Danvers, MA) to a protein concentration of about 3−5 mM in 50 mM MES buffer, pH 6.0. Atomic absorption measurements indicated full occupation of the metal site. The 2,3QD·flavonol complexes were prepared by anaerobic addition of the flavonols to a final concentration of 30 mM. As previously noted by Oka et al. for *A. flavus* 2,3QD (*14*), a bathochromic shift of the ~367 nm flavonolic band (367 nm → 380 nm in the case of quercetin) was observed by UV−vis spectroscopy upon incubation of the substrates with the enzyme. The samples were loaded into 1 mm thick polypropylene holders with Kapton foil windows and directly flash frozen in liquid nitrogen.

XAS Measurements. X-ray absorption spectra were recorded at 20 K at the D2 bending magnet beam line of the EMBL Outstation Hamburg at DESY. The synchrotron was operating at 4.5 GeV with ring currents ranging from 50 to 100 mA. A Si(111) double crystal monochromator and a focusing mirror with a cutoff energy of 21.5 keV were used throughout the study. The X-ray absorption spectra of the samples were recorded in fluorescence mode by means of a 13-element Ge solid-state detector (Canberra, Meriden, CT). EXAFS spectra were measured with ~0.4 eV steps in the edge region and 0.04 $Å^{-1}$ steps in the k range from 2 to 13 $Å^{-1}$. Integration times varied from 1 s in pre-edge region to 5 s at $k = 13$ $Å^{-1}$ for a total integration time of approximately 60 min/scan. Total exposure time per sample was typically 24 h. E_o and ΔE_o were 8983 and −6.6 eV, respectively.

Data Analysis. Data reduction based on standard methods (*22*) was performed with the local set of EXPROG programs (*23*). For each sample, the scans were inspected for edge consistency, normalized by the edge jump, and averaged. Only in the case of the native sample, a slight photoreduction of the metal was observed (see Supporting Information). However, this caused no significant change in the EXAFS region as determined by the analysis of individual scans. EXAFS spectra were extracted by subtracting the slowly varying atomic background fitted by three cubic splines. The raw EXAFS spectra were converted to k space and weighted by k^3 to compensate for the smaller amplitude at high k owing to the decay of the photoelectron wave. The analysis of the EXAFS spectra utilizing rapid curved multiple scattering

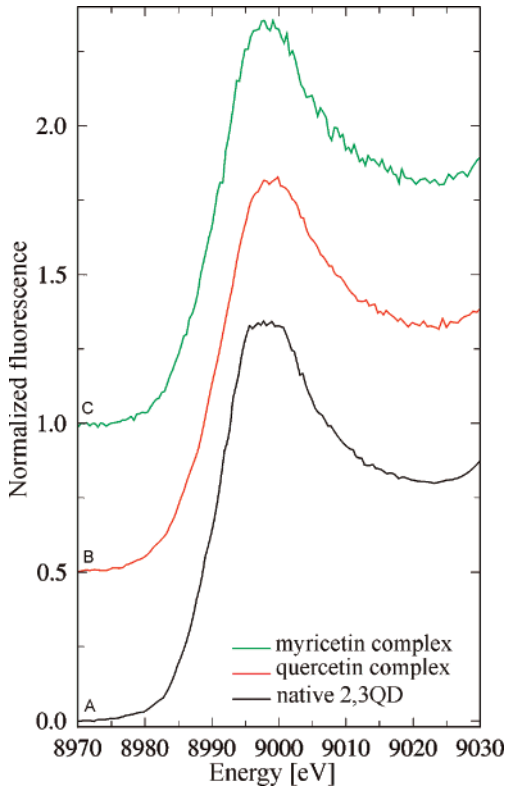

FIGURE 3: XANES spectra of (A) native 2,3QD, (B) 2,3QD in complex with quercetin, and (C) 2,3QD in complex with myricetin (5′-hydroxy quercetin).

theory was done with the program EXCURV98 (*24*). The positions of the peaks in the Fourier transform spectra were corrected for the phase shift of the closest ligand. The amplitude reduction factor was fixed at 1.0 for all fits. Fourier transforms were calculated in the k range of 3.0−12.0 Å^{-1}. The quality of the obtained fits was assessed by the fit index FI as defined by the software used

$$\mathrm{FI} = \sum_i [(\chi^{(i)}_{\mathrm{o}} - \chi^{(i)}_{\mathrm{c}})k^3]^2/n \times 100$$

where $\chi^{(i)}_{\mathrm{o}} - \chi^{(i)}_{\mathrm{c}}$ is the residual of point i, k is the value of the wavenumber at point i, and n is the number of experimental points. Multiple scattering calculations were applied to the imidazole ligands. The restrained refinement approach (*25*) was used.

RESULTS

XANES. The study of the XANES region is a powerful tool for probing the formal oxidation state of a metal owing to the great sensitivity of the edge position. In all samples discussed here, the XANES position and shape are conserved to a great extent and correspond to a formal Cu^{2+} oxidation state of the copper ion. The XANES pattern for the samples under study is plotted in Figure 3. They indicate that the complexes have similar metal coordination environments which differ from that of the native state.

EXAFS. The experimental and simulated EXAFS spectra of native 2,3QD as well as 2,3QD anaerobically complexed with the substrates QUE and MYR are shown in Figure 4 along with their corresponding Fourier transforms. A comparison of the different k-space spectra immediately reveals that the pattern of the native enzyme sample is different from

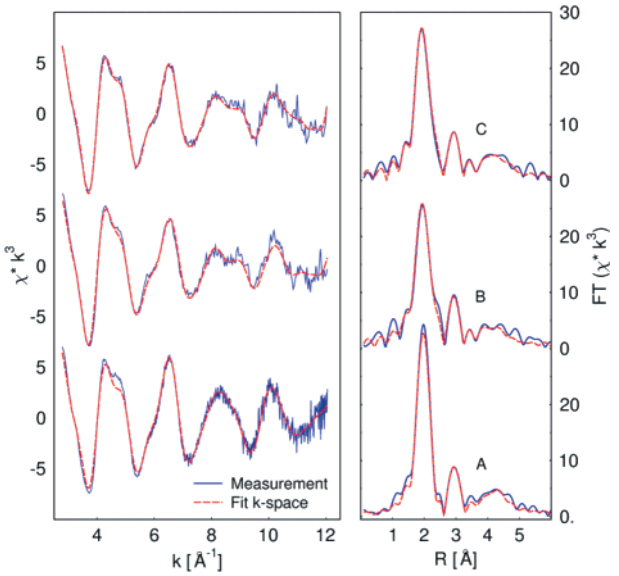

FIGURE 4: Experimental (blue) and simulated (red) EXAFS and Fourier transform spectra of (A) native 2,3QD, (B) 2,3QD in complex with quercetin, and (C) 2,3QD in complex with myricetin (5′-hydroxy quercetin).

those of the complexes. Furthermore, it can be noted that both anaerobic substrate complexes exhibit a virtually identical pattern. Compared to the native EXAFS, the complexes' spectra present a similar initial amplitude, but at about k = 8.5 Å^{-1}, a clear distinctive saddle occurs. Moreover, with increasing k, the signal is damped. As a result, the R-space Fourier transform spectrum of the as-isolated sample is dominated by a rather sharp single contribution at approximately 2.0 Å while the complexes' spectra show a decrease and broadening of the corresponding peak. Additional contributions, ascribable to higher shell scattering from the imidazole rings, are observed in all the Fourier transform spectra at longer distance. For the complexes, these contributions are of at least similar intensity to those observed in the native spectrum. This suggests the conservation of the histidine coordination upon substrate binding.

Simulation of the EXAFS Spectrum of 2,3QD. As mentioned earlier, the crystal structure shows that the copper coordination of *A. japonicus* 2,3QD is heterogeneous. The mononuclear copper center is mainly four-coordinated by His66, His68, His122, and a solvent molecule (Wat_{td}) with a distorted tetrahedral geometry. However, as a result of the alternative conformation of Glu73, a partial trigonal bipyramidal five-coordinated coordination (His66, His68, His122, Wat_{tb}, and Glu73) is also present at the metallocenter.

Taking advantage of the crystallographic results, four- and five-coordinated models constituted by three histidine residues and one or two oxygen atoms have been analyzed for consistency with the EXAFS measurements. As evidenced in Table 1, the fit of these models to the data results in an average copper−ligand distance of 2.01 Å and a Debye−Waller ($2\sigma^2$) parameter of 0.009 Å^2 for the single shell four-coordinated model (fit 1, 3His + 1O) and in a distance of 2.00 Å and a Debye−Waller parameter of 0.014 Å^2 for the five-ligands model (fit 2, 3His + 2O). In terms of the fit index (FI), the two models satisfy the data virtually equally well. FI is 0.493 for the four-coordinated model and only marginally lower for the five-coordinated model (FI =

Table 1: Curve-Fitting Results[a]

		first shell ligands				
	fit	His/O	R (Å)	$2\sigma^2$	FI	Figure
2,3QD	1	3/1	2.006(2)	0.009(1)	0.493	4A
	2	3/2	2.004(2)	0.014(1)	0.463	
2,3QD·QUE	3	3/1	2.006(4)	0.014(1)	1.105	4B
	4	3/2	2.006(3)	0.020(1)	0.732	
	5	3/3	2.006(13)	0.024(1)	0.849	
2,3QD·MYR	6	3/1	2.006(3)	0.013(1)	0.709	4C
	7	3/2	2.006(3)	0.019(1)	0.500	
	8	3/3	2.010(14)	0.024(1)	0.900	

[a] ΔE_o has been fixed to −6.6 eV for all refinements.

0.463). The distances obtained are fully consistent with copper−imidazole and copper−oxygen distances found in the Cambridge Structural Database (*26*). Whereas the Debye−Waller parameter refines for four ligands to a value typical for metalloenzymes with a rather ordered coordination sphere, it is quite at the upper boundary in the case of pentacoordination. The possibility of the existence of a split first shell was also explored. However, with an initial set of two distances (three His at 2.10 Å and two O at 1.96 Å and vice versa) the refinement converged to identical distances (2.00 Å) within the error. Thus, it seems that for the native enzyme the copper−ligand distances are fairly homogeneous.

Simulation of the EXAFS Spectra of the Complexes. Three possible coordination models were considered for fitting to the EXAFS data: a four-coordinated model (model A with 3N(His) + 1O), a five-coordinated model (model B with 3N(His) + 2O) and a six-coordinated model (model C with 3N(His) + 3O). In all models, we assumed that the three histidine ligands do not change upon substrate binding, in agreement with the similar histidine contributions present in the Fourier transforms of native and complexed 2,3QD at about 3.0 and 4.0 Å. Exploratory simulations with two imidazole units were unsatisfying. Proper simulation of the EXAFS amplitudes in the region 3.0 to 5.0 Å could only be achieved preserving the set of three histidine residues present in the native enzyme. Moreover, the imidazole rings appear to be rather rigid in all X-ray structure determinations reported so far (*9*) (also see companion paper) and are therefore unlikely to be displaced upon binding of the substrate.

A comparison of fittings 3 and 4 and 6 and 7 (Table 1) reveals that, differently from the native case, for both complexes, a first shell of five ligands (model B) is strongly favored over a four-ligand coordination (model A) as evidenced by the lower fit index (0.732 vs 1.105 in the case of 2,3QD·QUE and 0.500 vs 0.709 for 2,3QD·MYR). For both complexes, Model C (six-coordinated, fittings 5 and 8 for 2,3QD·QUE and 2,3QD·MYR, respectively) can be ruled out because of its worse fit index (0.849 and 0.900 for 2,3QD·QUE and 2,3QD·MYR, respectively).

The five-coordinated model yielded for both complexes an average distance identical to that of the native sample (2.00 Å). However, it is accompanied by much higher Debye−Waller parameters (0.020 Å^2 for the 2,3QD·QUE sample (fit 4) and 0.019 Å^2 for the 2,3QD·MYR sample (fit 7)). This suggests that most likely two or more shells of ligands are present. This possibility has been investigated. The refinement of two shells of ligands produced in the case of 2,3QD·QUE one contribution at about 1.96 Å and the other at 2.05 Å. Very similar distances were obtained in the case of 2,3QD·MYR. Although these results seem indeed to indicate the existence of two close distinct shells of ligands, we do not believe that the available data (up to 12 Å^{-1}) range justifies such a resolution. We therefore conclude that in the complexes a possibly quite broad distribution of ligands centered at 2.00 Å is present.

DISCUSSION

Although exact mechanistic information on 2,3QD-mediated dioxygenation of flavonols is lacking, the early biochemical study on *A. flavus* 2,3QD (*14*) and subsequent biomimetic studies (*15*, *18*−*21*) have suggested the general features of a possible mechanism for the enzymatic dioxygenation reaction (Figure 5). The first step is believed to be the binding of the flavonol substrate to the copper ion (structure **2**). Subsequently, the activated flavonol form (**3**) is assumed to be attacked at the C2 atom by the dioxygen molecule. The peroxide produced cyclizes to form an endoperoxide (**4**) which decomposes releasing the products (**5**) and regenerating the native enzyme (**1**). In this XAS study, we have investigated structures **1**−**3** of this reaction scheme.

Native Enzyme (1). The crystal structure of 2,3QD has evidenced the existence of a heterogeneous copper environment (*9*). At pH 5.2, the copper center displays a mixed four- (principal) and five-coordination (Figure 2). Our present EXAFS analysis confirms that native 2,3QD is indeed equally well-described by a shell of either four or five low-Z

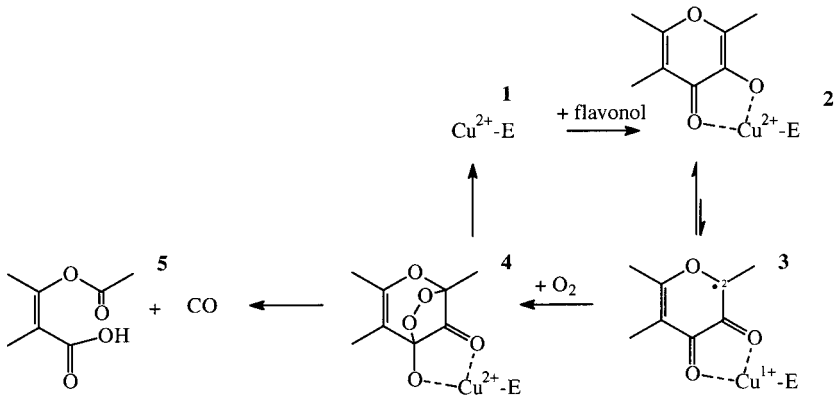

FIGURE 5: Schematic representation of a possible mechanism of 2,3QD-mediated dioxygenation of flavonols as derived from model studies on copper flavonolate-catalyzed dioxygenation of 3-hydroxy flavone (*15*).

scatterers positioned at an average distance of 2.00/2.01 Å, respectively, from the copper center. Standard bond valence summation (BVS) calculations (*27*, *28*) also support the idea of a mixed coordination. Because errors in a BVS calculation are approximately ±0.25 units, it is generally accepted that, for a divalent site and good agreement, a BVS calculation should produce values in the range of 1.75−2.25. Although a BVS analysis does not have an absolute value and a number of examples have been found of complexes deviating from the predicted behavior (*26*), BVS calculations remain a useful tool to detect possible major coordination irregularities. In the case of 2,3QD, the five-coordination BVS calculation results in a value of 2.28, which is marginally on the upper limit of the range, indicating a rather crowded shell for the given distance of 2.00 Å. On the other hand, for the four-coordinated model, we obtained a BVS value of 1.89 which properly matches the aforementioned condition. Therefore, although the accuracy in determining the coordination number from a XAS measurement is generally not very high, particularly in the absence of pre-edge features, the consistency of our results both in terms of fit index and BVS analysis increases our confidence in suggesting that, in solution, as well as in the crystalline state, an average coordination number intermediate between four and five describes the copper site of 2,3QD the best.

Agreement with the crystallographic result is also found for the metal−ligand distances, although a few differences are present. The average metal−ligand distance in the crystal structure is 2.15 Å. Distances range from 2.09 (Cu−His68$^{N\epsilon 2}$) to 2.41 Å (Cu−Wat$_{tb}$) (see Figure 2) with rms differences between the four 2,3QD molecules in the asymmetric unit in the order of 0.1 Å. The only outlier is the longest distance (Cu−Wat$_{tb}$) for which the rms difference amounts to 0.2 Å. The EXAFS fittings for the native enzyme suggest an average distance of 2.00 Å, which is shorter that that proposed by X-ray crystallography. This difference can be explained considering the uncertainties inherent to the different structural probes, the different pH value, and temperature of the experiments (pH 5.2 and 100 K in the crystallographic determination and pH 6.0 and 20 K in the XAS measurement), and possibly a photoreduction effect. The higher pH and lower temperature used in the XAS measurement are consistent with the somewhat shorter distances from the EXAFS analysis. Some photoreduction, which presumably has occurred in the course of the high-resolution crystallographic data collection of native 2,3QD to an extent higher than that observed in the course of the XAS measurement (see Supporting Information), is also consistent with the overall longer crystallographic metal−ligand average distance. However, we stress that photoreduction cannot account for the double coordinating conformation observed in the crystallographic structure as EPR measurements on native 2,3QD evidence a multiple spectral line (*9*). We have no evidence for a scatterer in the 2.4 Å region, as seen in the X-ray structure. This might be caused by the partial occupancy of the ligand at this distance (Wat$_{tb}$). On the other hand, the high variability exhibited by the Cu−Wat$_{tb}$ distance in the X-ray structure leaves the possibility open for an overall shorter Cu−Wat interaction.

*Anaerobic E·S Complexes (**2**, **3**).* The present EXAFS study shows that the binding of QUE and MYR occurs under anaerobic conditions and that it has clear geometric effects on the copper coordination. As evidenced by the results reported in Table 1, the best EXAFS fit of 2,3QD·QUE is obtained for a five-coordinated Cu site of low-Z scatterers located at an average distance of 2.00 Å. The identical fit of 2,3QD·MYR suggests that the 5′-hydroxyl group in myricetin does not modify substrate positioning at the metallocenter. This is consistent with the very similar rate at which these substrates are degraded (*14*).

In consideration of the active site shape (*9*), the best set of ligands (3His + 2O) might arise from a unique arrangement in which His66, His68, His112, Glu73, and flavonol provide the Cu-coordinating ligands. The oxygen atoms from the Glu73 carboxylate and from the flavonol molecule each bind as a monodentate ligand. The water molecule present in the native structure as a ligand is displaced by the binding of the substrate. This is a reasonable assumption as the shape of the active site cavity dictates that the water molecule must be removed from the coordination sphere upon flavonol ligation (*9*). Water displacement is also observed in the crystal structures of 2,3QD inhibited by dietyldithiocarbamate and kojic acid (see companion paper).

Despite the known chelating capability of flavonols (*15*, *29*), monodentate flavonol ligation through the 3−OH has an interesting functionally relevant precedent in model systems. Nishinaga et al. (*30*) have shown that some flavonols bind to [Co^{3+}−(salen)(OH)] to form monodentate flavonolatocobalt complexes which are susceptible to oxygenation in coordinating solvents such as DMF. While it is not clear why in the model compound flavonol monodentate coordination is preferred, in 2,3QD it is dictated by the active site geometry and protein environment which stabilize this geometry the best (*9*). The second oxygen atom of the ligand sphere can only be provided by the carboxylate group of Glu73 because no other O donor is available (*9*). In terms of distances, a Cu−Glu73$^{O\epsilon 1}$ interaction of 2.00 Å is in good agreement with the average Cu−O^{carboxylate} distance of 1.96 Å found in small molecules (*31*).

CONCLUSIONS

The coordination properties of the catalytic center of the intriguing copper-dependent *A. japonicus* quercetin 2,3-quercetinase have been elucidated by XAS spectroscopy. In line with the previously proposed mechanism (Figure 5), we observe that binding of quercetin to the copper center does not require an aerobic environment and that binding does not alter the Cu^{2+} oxidation state of the resting enzyme. Under anaerobic conditions, the proposed tautomeric Cu^{+} activated complex (**3**) with a C2 carbon-centered radical represents, therefore, most likely only a minor form. This appears to be a sensible mechanism to control the formation of highly reactive centers. Model studies on a Cu^{2+} complex of flavonolate and 3,3′-imino-bis(*N*,*N*-dimethylpropylamine) (*20*) are in agreement with an asymmetric equilibrium which favors the Cu^{2+} state. The unique occurrence of a carboxylate bound to the copper ion is consistent with its key functional role (*9*) and suggests that the glutamate residue likely play a role in the fine-tuning of this equilibrium (see companion paper). Research aimed at a better understanding of the mechanistic aspects of this intriguing enzyme reaction is currently ongoing.

SUPPORTING INFORMATION AVAILABLE

XANES spectra of the different samples after 1 and 24 h of exposure to the X-rays. This material is available free of charge via the Internet at http://pubs.acs.org.

REFERENCES

1. Hayaishi, O. (1974) in *Molecular Mechanisms of Oxygen Activation* (Hayaishi, O., Ed.) pp 1−28, Academic Press, New York.
2. Broderick, J. B. (1999) *Essays. Biochem. 34*, 173−189.
3. Hamilton, G. A. (1974) in *Molecular Mechanisms of Oxygen Activation* (Hayaishi, O., Ed.) pp 405−451, Academic Press, New York.
4. Bairoch, A. (1993) *Nucleic Acids Res. 21*, 3155−3156.
5. Boldt, Y. R., Sadowski, M. J., Ellis, L. B. M., Que, L., Jr., and Wackett, L. P. (1995) *J. Bacteriol. 177*, 1225−1232.
6. Gibello, A., Ferrer, E., Martin, M., and Garrido-Pertierra, A. (1994) *Biochem. J. 301*, 145−150.
7. Oka, T., and Simpson, F. J. (1971) *Biochem. Biophys. Res. Commun. 43*, 1−5.
8. Hund, H. K., Breuer, J., Lingens, F., Huttermann, J., Kappl, R., and Fetzner, S. (1999) *Eur. J. Biochem. 263*, 871−878.
9. Fusetti, F., Schröter, K. H., Steiner, R. A., van Noort, P. I., Pijning, T., Rozeboom, H. J., Kalk, K. H., Egmond, M. R., and Dijkstra, B. W. (2002), *Structure 10*, 259−268.
10. Hattori, S., and Noguchi, I. (1959) *Nature 184*, 1145−1146.
11. Bartz, W. (1971) *Arch. Mikrobiol. 78*, 341−352.
12. Oka, T., Simpson, F. J., Child, J. J., and Mills, C. (1971) *Can. J. Microbiol. 17*, 111−118.
13. Child, J. J., Simpson, F. J., and Westlake, D. W. S. (1963) *Can. J. Microbiol. 9*, 653−664.
14. Oka, T., Simpson, F. J., and Krishnamurty, H. G. (1972) *Can. J. Microbiol. 18*, 493−508.
15. Speier, G. (1991) in *Dioxygen activation and homogeneous catalytic oxidation* (Simándi, L. I., Ed.) pp 269−278, Elsevier Science Publishers B. V., Amsterdam, The Netherlands.
16. Balogh-Hergovich, E., Speier, G., and Argay, G. (1991) *J. Chem. Soc., Chem. Comm.* 551−552.
17. Balogh-Hergovich, E., Kaizer, J., Speier, G., Huttner, G., and Zsolnai, L. (2000) *Inorg. Chim. Acta 304*, 72−77.
18. Balogh-Hergovich, E., Kaizer, J., and Speier, G. (2000) *J. Mol. Catal. 159*, 215−224.
19. Barhács, L., Kaizer, J., and Speier, G. (2001) *J. Mol. Catal. 172*, 117−125.
20. Barhács, L., Kaizer, J., Pap, J., and Speier, G. (2001) *Inorg. Chim. Acta 320*, 83−91.
21. Kaizer, J., and Speier, G. (2001) *J. Mol. Catal. 171*, 33−36.
22. Scott, R. A. (1985) *Methods Enzymol. 111*, 414−459.
23. Nolting, H. F., and Hermes, C. (1992) EXPROG: EMBL EXAFS data analysis and evaluation program package for PC/AT, European Molecular Biology Laboratory c/o DESY, Hamburg, Germany.
24. Binsted, N., and Hasnain, S. S. (1996) *J. Synchrotron Rad. 3*, 185−196.
25. Binsted, N., Strange, R. W., and Hasnain, S. S. (1992) *Biochemistry 31*, 12117−12125.
26. Allen, F. H., Bellard, S., Brice, M. D., Cartwright, B. A., Doubleday, A., Higgs, H., Hummelink, T., Hummelink-Peters, B. G., Kennard, O., Motherwell, W. D. S., Rodgers, J. R., and Watson, D. G. (1979) *Acta Crystallogr., Sect. B 35*, 2331−2339.
27. Brown, I. D., and Altermatt, D. (1985) *Acta Crystallogr., Sect. B 41*, 244−247.
28. Liu, W., and Thorp, H. H. (1993) *Inorg. Chem. 32*, 4102−4105.
29. Balogh-Hergovich, E., Kaizer, J., Speier, G., Huttner, G., and Jacobi, A. (2000) *Inorg. Chem. 39*, 4224−4229.
30. Nishinaga, A., Kuwashige, T., Tsutsui, T., Mashino, T., and Maruyama, K. (1994) *J. Chem. Soc., Dalton Trans.* 805−810.
31. Harding, M. M. (1999) *Acta. Crystallogr., Sect. D 55*, 1432−1443.
32. Addison, A. W., Hendriks, H. M. J., Reedijk, J., and Thompson, L. K. (1981) *Inorg. Chem. 20*, 103−110.
33. Kraulis, P. (1991) *J. Appl. Crystallogr. 24*, 946−950.
34. Merritt, E. A., and Bacon, D. J. (1997) *Methods Enzymol. 277*, 505−524.

BI015974Y